International Journal of Refractory Metals and Hard Materials 116 (2023) 106362

Contents lists available at ScienceDirect

International Journal of Refractory Metals and Hard Materials

journal homepage: www.elsevier.com/locate/IJRMHM

Analysis of wear mechanism and sawing performance of carbide and PCD circular saw blades in machining hard aluminum alloy

Jinyou Kang [a,b], Jinsheng Zhang [a,b,*], Kaida Wang [a,b], Dongfang Zhang [a,b], Tianyu Bai [a,b], Heng Zhang [a,b], Weiye Song [a,b]

[a] Key Laboratory of High-Efficiency and Clean Mechanical Manufacture, Ministry of Education, School of Mechanical Engineering, Shandong University, Jinan 250061, China

[b] Rizhao Research Institute, Shandong University, Rizhao 276800, China

ARTICLE INFO

Keywords:
Circular saw blade
High-speed sawing
Wear mechanism
Sawing performance
Tool wear

ABSTRACT

High-efficiency sawing is widely applied in primary and secondary machining sectors, but it faces limitations due to saw tooth life and manufacturing constraints. This research investigates the wear mechanism, wear characteristics, and sawing performance of carbide and polycrystalline diamond (PCD) saw teeth when machining hard aluminum alloy. The results show that the sawing forces with PCD saw teeth are less than those of carbide teeth, yielding better surface quality and longer tool life. The wear mechanisms of saw teeth of two materials with different tooth types are classified and characterized finely. Carbide teeth are subject mainly to abrasion and adhesion at the cutting edges, while adhesion, corrosion, and diffusion primarily contribute to flank face wear. PCD teeth mainly suffer from abrasion and micro-chipping on the cutting edges and faces. A comprehensive description of the wear evolution of carbide and PCD teeth is presented, with the cutting heat being the primary cause of carbide tooth wear and the presence of hard particles in the workpiece causing PCD tooth wear by SEM and EDS analysis. The friction coefficient of the PCD teeth is considerably lower than that of the carbide teeth by sliding friction and wear tests, which also proves its more superior thermal stability and wear resistance during wear evolution analysis. Systematic research analyzes and discusses the wear mechanism and wear characteristics of saw teeth in high-speed sawing process, which can further enhance the understanding of the saw tooth wear to provide theoretical guidance for saw tooth design and manufacturing.

1. Introduction

7075 aluminum alloys, a cold-treated forged alloy, possesses exceptional hardness and surpasses common metals in terms of strength. It stands as a superior alloy, possessing outstanding mechanical properties, corrosion resistance, and a high potential for commercial utilization [1]. This alloy finds representation in various industries, including aerospace, mold machining, mechanical equipment, as well as jigs and fixtures. Its remarkable strength and corrosion resistance make it an ideal choice for manufacturing aircraft structures and other high-stress structural components [2,3]. Carbide circular saw blades play an indispensable role in the metal sawing industry, particularly for hard aluminum alloy ingots. The tools serve as the starting point for material processing and find extensive application in workpiece grooving, cut-off operations, and other crucial processes [4,5]. Based on their geometry, saw tooth structures are broadly categorized as rougher teeth and finisher teeth. The component of the carbide tooth material used is shown in Table. 1 in this paper. Fig. 1 illustrates the wear trace process of carbide teeth. Due to their exceptional hardness and wear resistance, both carbide and polycrystalline diamond (PCD) are widely employed as tooth materials for circular saw blades [6,7]. Numerous researchers have devoted their efforts to studying the saw tooth wear and sawing stability of circular saw blades [8,9]. Currently, addressing the challenges related to extending the service life of saw teeth, improving machining efficiency, and enhancing the quality of the machined surface is of utmost importance. This work aims to achieve an in-depth understanding of the wear mechanism and wear evolution of carbide and PCD teeth during hard metal sawing.

In essence, metal sawing involves the plastic removal of materials through the intermittent cutting using saw teeth. However, the saw teeth

* Corresponding author at: Key Laboratory of High-Efficiency and Clean Mechanical Manufacture, Ministry of Education, School of Mechanical Engineering, Shandong University, Jinan 250061, China.
E-mail address: zhangjs@sdu.edu.cn (J. Zhang).

https://doi.org/10.1016/j.ijrmhm.2023.106362
Received 8 June 2023; Received in revised form 8 August 2023; Accepted 8 August 2023
Available online 9 August 2023

Table 1
Composition of carbide saw tooth used in this paper.

Element	Co	Cr	W	C	O
Wt%	82.63	0.55	0.93	14.50	1.09

inevitably experience wear, which manifests in various forms including adhesive, corrosive, abrasive, cracking, and chipping wear [8,10]. The high hardness of the workpiece material leads to substantial cutting forces and severe abrasive wear at the tool-chip interface. Additionally, the lower thermal conductivity of the interface increases the cutting temperature, further exacerbating the wear and potential failure of carbide tools. These failure modes encompass adhesive wear, oxidative wear, and diffusive wear [11]. The utilization of the PCD tool material offers unique advantages, particularly its exceptional physic-mechanical properties, especially at high temperatures. The PCD exhibits high wear resistance, super-hardness, and relatively low chemical reactivity with various metallic materials [12,13]. Consequently, the PCD tools are well-suited for machining super-hard materials. Furthermore, the PCD tools possess a significantly longer service life compared to conventional carbide tools, resulting in saved time due to reduced tool switching and enhanced machining efficiency [14].

The issue of tool wear in metal machining has been extensively researched, particularly in the context of turning or milling operations. Many scholars have dedicated their efforts to studying the progression of tool wear, with a particular focus on carbide tools [15–17], ceramic tools [18,19], as well as PCD or CBN coated tools [20–22]. In the pursuit of understanding phase-related tool wear, experiments were conducted involving the turning of Ti-6Al-4 V using PCD and carbide inserts, allowing for a comparison between PCD tools and WC-6Co tools [23]. Evaluating the performance of an experimental carbide insert, Ventura [24] examined the impact of edge preparation. Interestingly, it was revealed that neither the experimental nor numerical temperatures of the chips or the tool-chip interface had a direct correlation with the edge preparation. Li [25] undertook a comprehensive modeling study to elucidate the wear mechanism and tribological behavior of PCD tools during the cutting of Ti6Al4V. The investigation highlighted the influence of the stress distribution and the type of PCD material on the distinctive shape and morphology of wear areas. Furthermore, Calatoru [3] delved into the diffuse wear mechanism of carbide end mills employed in high-speed machining of 7475-T7351 aluminum alloy. The study brought to light an unusual and previously unknown manifestation of diffuse wear, which poses challenges for manufacturers seeking to fully leverage the potential of tungsten carbide tools in the high-speed machining of aerospace aluminum. Liu [26] made significant contributions to the field of tool wear, conducting a comprehensive study on the effects of tool breakage and wear on cutting forces. The aim was to enable tool condition monitoring and facilitate smart manufacturing practices. Carbide circular saw blades have gained renown for their exceptional resistance to abrasive wear. However, their high hardness renders them susceptible to fracture under high-impact loads, particularly when cutting cobalt-based high-temperature alloys. Developing high-performance circular saw blades necessitates a profound understanding of practical applications. It is crucial to recognize that sawing tribological systems are unique, where even minor variations in system parameters can lead to fundamental changes in wear rates and wear mechanisms. Sheikh-Ahmad [27] conducted a comprehensive study on the wear of tungsten carbide tools during the cutting of particle boards at different speeds, utilizing a high-speed lathe. Lu [28] delved into the fabrication of micro-textures on saw teeth to evaluate their impact on the cutting performance of circular saw blades. Lewis [29] conducted an analysis of the effect of surface treatment on the wear and failure behavior of TiN-coated HSS circular saw blades. There is considerable research on sawing wood with carbide circular saw blades, whereas the investigation of wear characteristics of saw teeth in the field of metal sawing remains relatively limited [4,30]. Therefore, further analysis and comprehensive studies are warranted to deepen our understanding of the wear mechanisms and sawing performance of both carbide and PCD

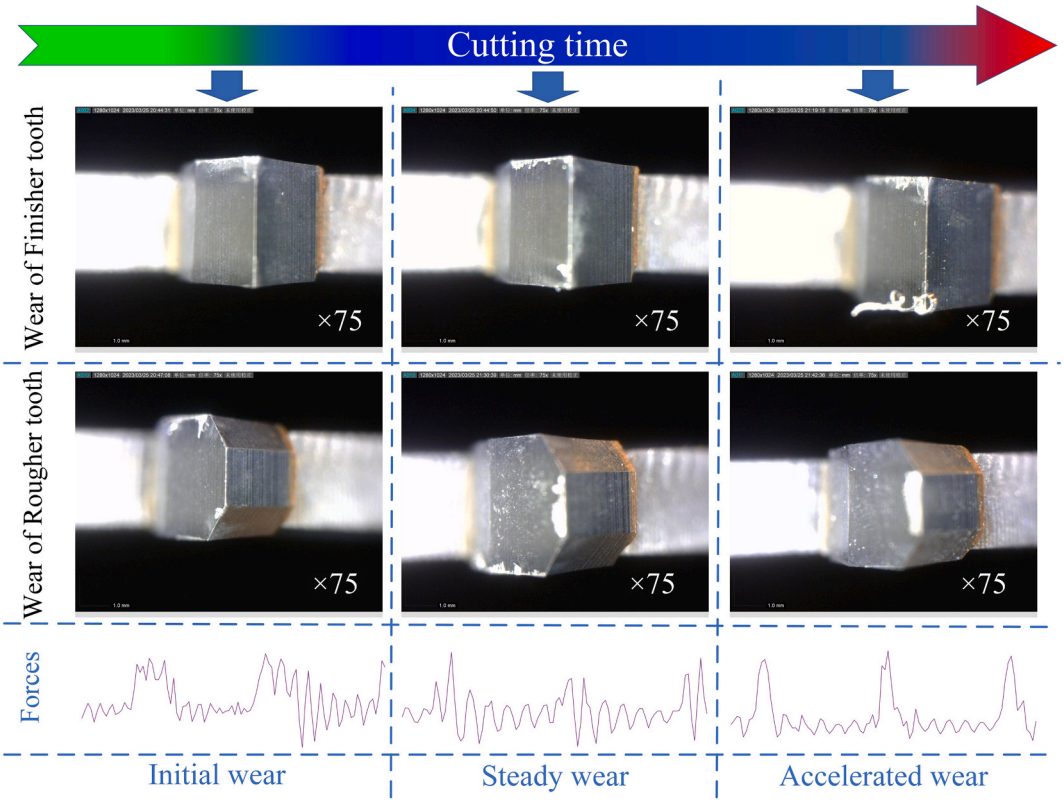

Fig. 1. Wear process of the finisher tooth and rougher tooth.

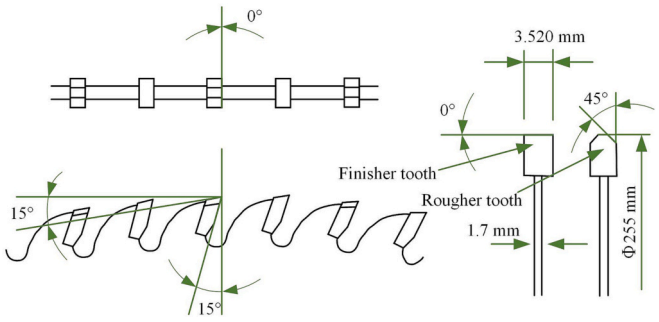

Fig. 2. Basic geometry parameters of the saw tooth.

teeth.

In this study, a holistic investigation is conducted to characterize the wear morphology and behavior of carbide and PCD teeth based on sawing experiments of the hard aluminum alloy. The objective is to present a detailed understanding of the wear mechanisms associated with different saw tooth materials. Scanning electron microscopy (SEM) is employed to analyze the wear microstructures, enabling the identification of key factors contributing to wear. The wear behaviors of different zones of the saw teeth are systematically classified and summarized more finely. A comparative analysis of the wear micrographs between carbide and PCD teeth provides valuable insights into the distinctive wear damage mechanisms exhibited for these materials. Finally, a comprehensive depiction of the evolution of the saw tooth wear is presented, offering a deeper understanding of the underlying wear behavior.

2. Experimental details

2.1. Preparation of circular saw blades

The geometric dimensions of the carbide and PCD circular saw blades used in this experimental design are depicted in Fig. 2. The circular saw blade has an outer diameter d_s of 255 mm and an inner diameter of 32 mm. Each blade is equipped with 48 teeth (Heyuan Fuma Carbide Co., Ltd. in China), comprising 24 rougher and 24 finisher teeth, which are alternately welded to the outer diameter of the circular saw blade. The PCD layer has a thickness of 0.72 mm. The circular saw blade body is made of 75Cr1 alloy steel, with the modulus of elasticity is 209 GPa, the density is 7800 kg/m^3, and the poisson's ratio is 0.3. To mitigate potential errors and random factors associated with the tooth wear, three carbide circular saw blades and two PCD circular saw blades were prepared for the sawing experiments.

2.2. Experimental setup

Sawing experiments were performed on a high-precision Daewoo ACE-V500 CNC milling machine (Fig. 3), which features a variable speed range of 80 to 10,000 r/min. The circular saw blade was securely fastened using an 88 mm diameter flange plate. The sawing material utilized in this study is a high-hardness 7075 aluminum alloy, with the following material properties: young's modulus of 71.1 GPa, yield strength of 455 MPa, and tensile strength of 524 MPa. The dimensions of the workpiece for this experiment are 100 mm × 100 mm × 65 mm, and the specific sawing length is set at 100 mm. The sawing parameters employed in this research are fixed with the following values: the sawing rotational speed of 3000 r/min, the feed rate of 400 mm/min, and the depth of cut a_p of 25 mm. Throughout the sawing process, the sawing fluid (solcut oil—V600, DOMINO Co. Ltd., China) was continuously supplied at a flow rate of 11.21 L/min.

To evaluate the tooth wear, the rake and flank faces of the saw teeth were measured after every two sawing passes using an optical microscope. To minimize measurement errors, multiple teeth were measured, and each wear observation was repeated three times. The average value was taken as the wear value. The sawing force was measured using a Kistler piezoelectric dynamometer (Type 9257B) mounted on the machine table, as depicted in Fig. 3(b). After the experiments, the saw teeth were extracted via the laser cutting and examined using SEM (SU-70) and confocal microscopy (LSM 800). Finally, the machined surface of the workpiece and the chips were collected for observation.

Additionally, the friction and wear tests of samples of the carbide tooth, PCD layers and workpieces of the same material were conducted with a ball on a disc on a flat surface (UMT-2, Tribology Center Inc., USA). The 304 stainless steel ball with a diameter of 9.25 mm was applied as the face material of the flat specimen at 15 N normal load, 6 mm/s linear sliding speed, and 5 mm wear track length. The tests were

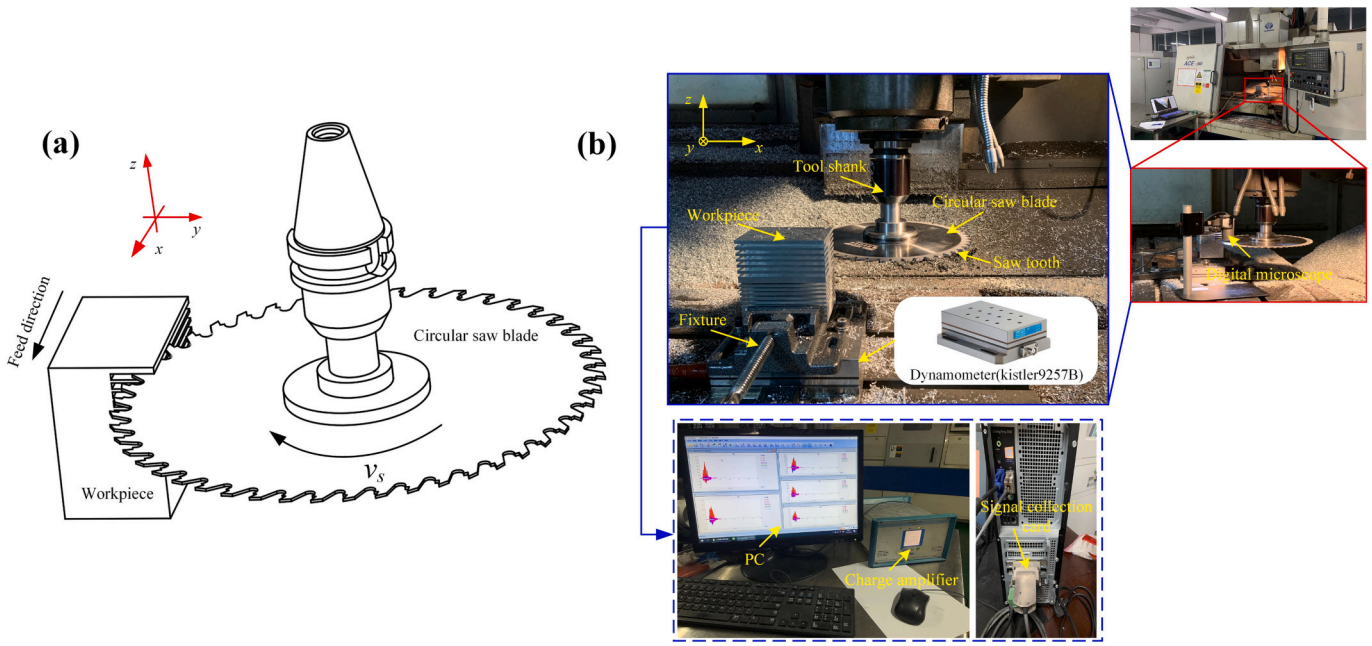

Fig. 3. Schematic diagram and sawing experimental setup.

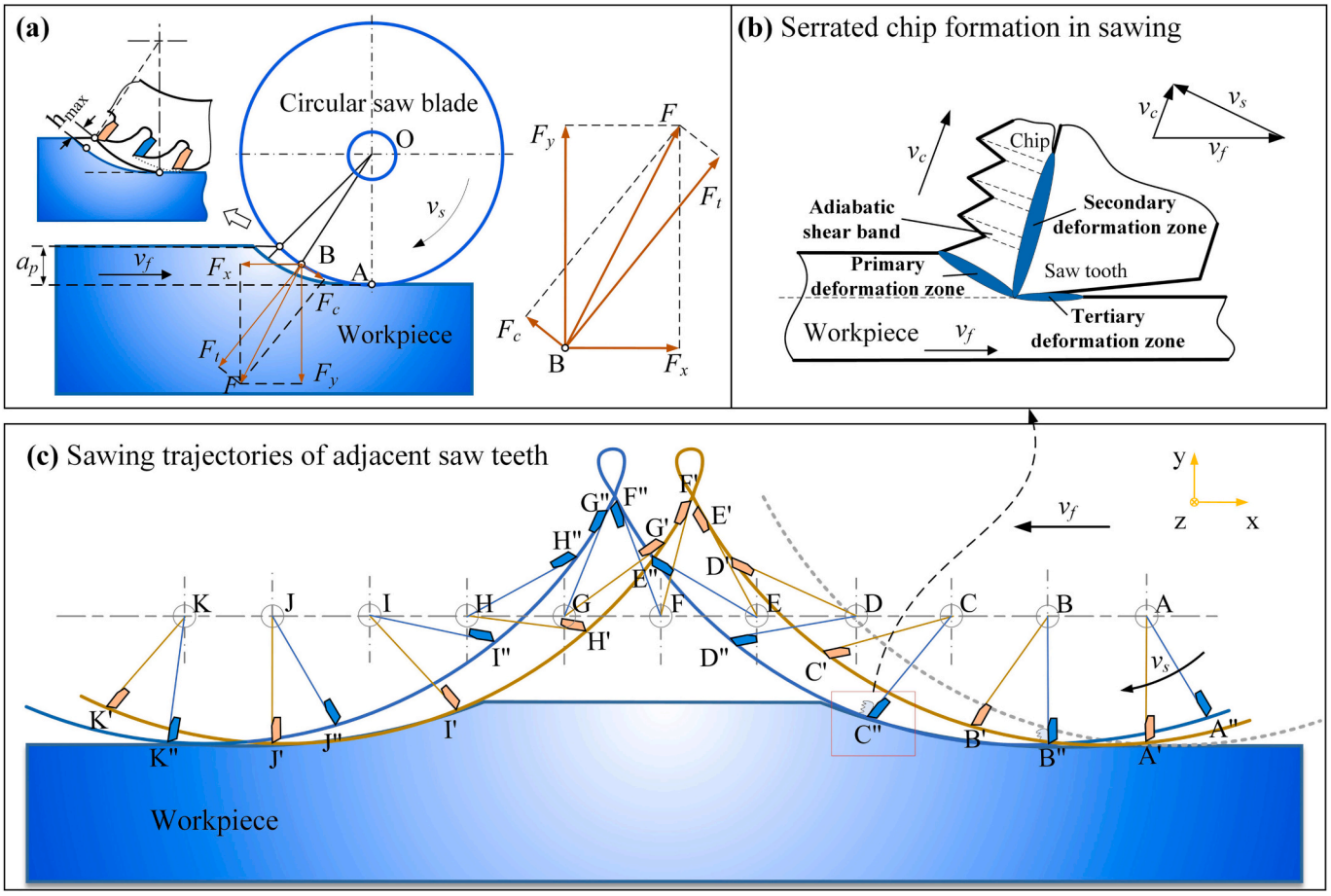

Fig. 4. (a) Sawing geometry; (b) serrated chip formation in sawing; (c) sawing trajectories of adjacent saw teeth.

executed at room temperature. The friction and wear measurement cycle was 15 min, and each group of all samples was operated three times to eliminate the accidental errors of data collection in testing and ensure the effectiveness of the results.

3. Results and discussion

3.1. Sawing forces in machining hard aluminum alloy

Sawing forces play a critical role in monitoring the wear condition of saw teeth and understanding the wear mechanism [31,32]. The service life of saw teeth directly impacts the cost of circular saw blade tools. Various forms of wear, such as adhesion, oxidation, chipping, corrosion, cracking, and delamination, occur in saw teeth and are closely associated with the contact stress in the sawing zone. Therefore, a comprehensive understanding of relevant parameters and contact stresses of the saw teeth is essential for the sawing process. However, directly measuring the contact stresses between the saw tooth and the workpiece is challenging.

To gain insights into the sawing process and investigate the wear mechanism of the saw teeth, a detailed depiction of the sawing process is presented in Fig. 4. Fig. 4(a) illustrates the forces acting on the circular saw blade during the intermittent sawing, where the position of the combined force varies periodically with the number of saw teeth within the sawing arc. Fig. 4(b) demonstrates the formation of serrated chips during sawing, with the rate of formation being influenced by the feed rate and rotational speed [33]. Considerable cutting heat is generated at the cutting edge and the tool faces [34]. The trajectories of adjacent saw teeth during the sawing process are depicted in Fig. 4(c). The thickness of the chips is determined by the interaction between two adjacent saw teeth. Moreover, the machined surface is influenced by the lateral vibration of the saw teeth [35], resulting in lamination and rubbing damage on the machined surface.

During the sawing process, the sawing forces in three directions were recorded. To assess the impact of carbide and PCD teeth on the circular saw blade, the sawing forces during the steady sawing phase were statistically analyzed using MATLAB software to facilitate convenient comparisons. Fig. 5 illustrates the three components of sawing forces for carbide and PCD teeth (the 1st sawing). From Fig. 5(a), it is evident that the sawing force waveform exhibits periodicity, which is a characteristic of intermittent sawing. Comparing Fig. 5(a) and (b), it is noticeable that the sawing force exerted by the PCD tooth in the feed direction is significantly lower than that of the carbide tooth. Under the same conditions, the sawing force in the depth-of-cut direction can be reduced by more than 45 N, as evident from the comparison between Fig. 5(c) and (d). Similarly, the sawing force in the axial direction can be reduced by over 50 N under the corresponding conditions. The results of the sawing force analysis in the three directions indicate that the circular saw blade with PCD teeth achieves a notable reduction in sawing forces, which can be attributed to the lower chemical activity between the PCD teeth and the workpiece material. This finding underscores the potential of PCD teeth in the field of sawing metal materials, particularly aluminum alloys.

In automated manufacturing, the sawing forces serve as valuable indicators for monitoring the sawing process and the tool's working condition. Throughout the initial, steady, and accelerated wear phases, the sawing forces exhibit constant variations, as depicted in Fig. 6. The variations in maximum sawing force for carbide and PCD circular saw blades are recorded in different directions for the 1st, 5th, 10th, 15th, 20th and 25th occurrences. Given that the sawing process involves

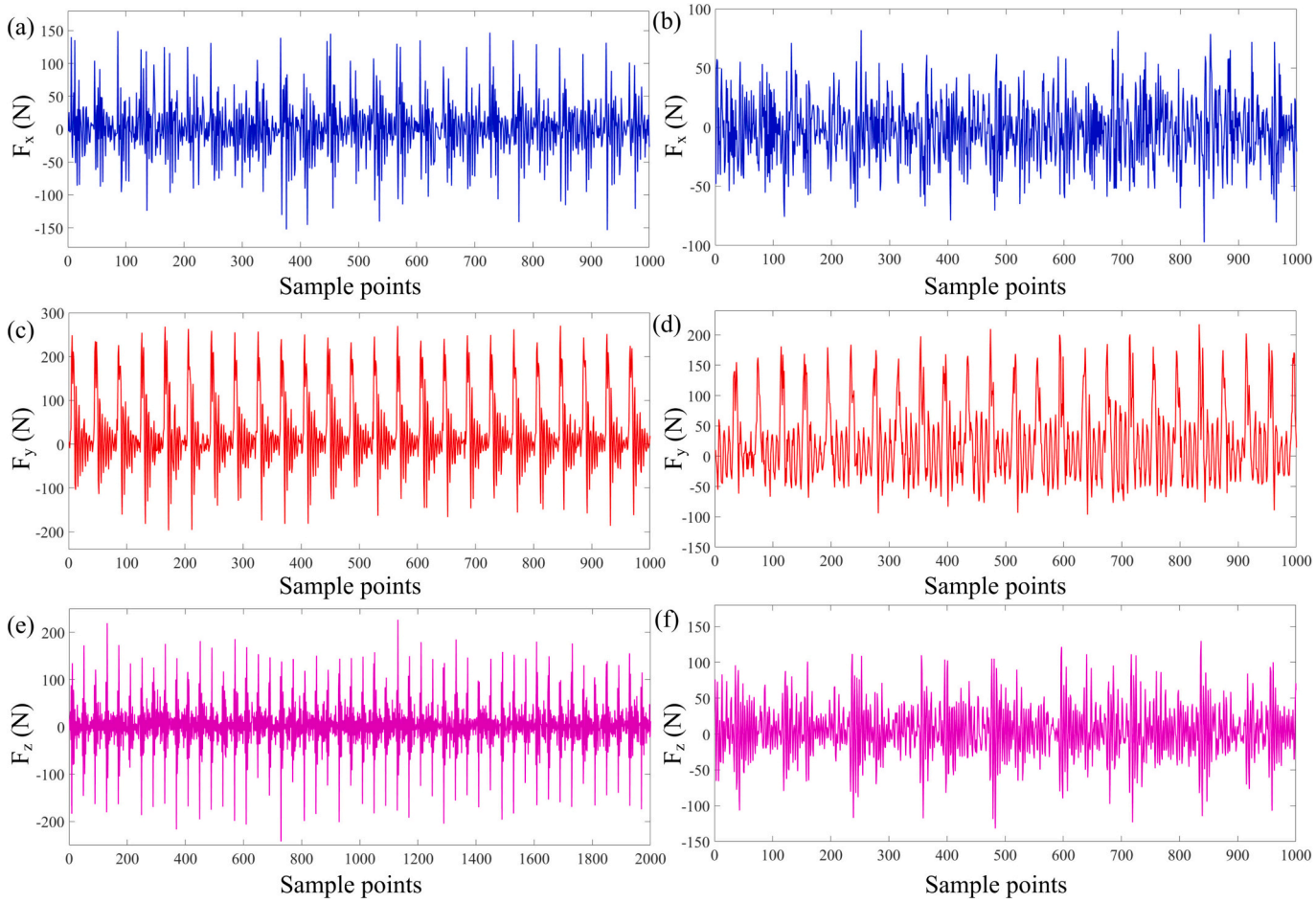

Fig. 5. Sawing force waveforms in different directions for (a), (c), (e): carbide and (b), (d), (f): PCD teeth (the 1st sawing).

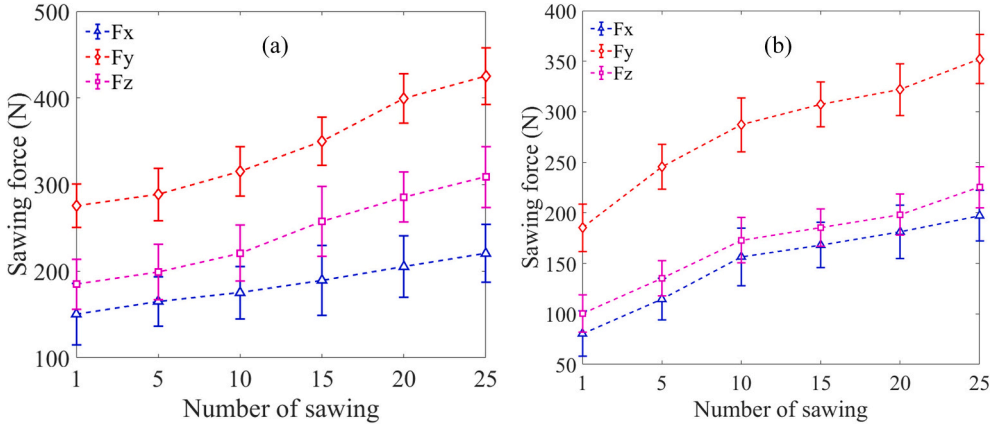

Fig. 6. Variation of sawing forces with the number of sawing times using (a) carbide teeth and (b) PCD teeth.

rough machining, the maximum value of sawing force variation may exhibit some degree of error. In general, the sawing force demonstrates an increasing trend as the number of sawing occurrences. From the analysis of Fig. 6, the maximum axial force F_z is larger than the force F_x in the feed direction and lower than the sawing force F_y in the depth-of-cut direction, which may be related to the horizontal type sawing way. Experimental verification will be performed using the sawing machine in future studies.

3.2. Wear analysis of carbide and PCD teeth

The wear values of different sawing faces were periodically observed and measured using an optical microscope during the sawing experiments. As mentioned earlier, the PCD layer enhances the capability of sawing hard aluminum alloys. This leads to an extended tool life for PCD teeth in comparison to carbide teeth, as depicted in Fig. 7. It is evident that the wear trends of carbide and PCD teeth are similar. Initially, the flank face wear is more pronounced, but subsequently, the wear of the saw teeth becomes relatively stable. At the 23rd sawing occurrence, the

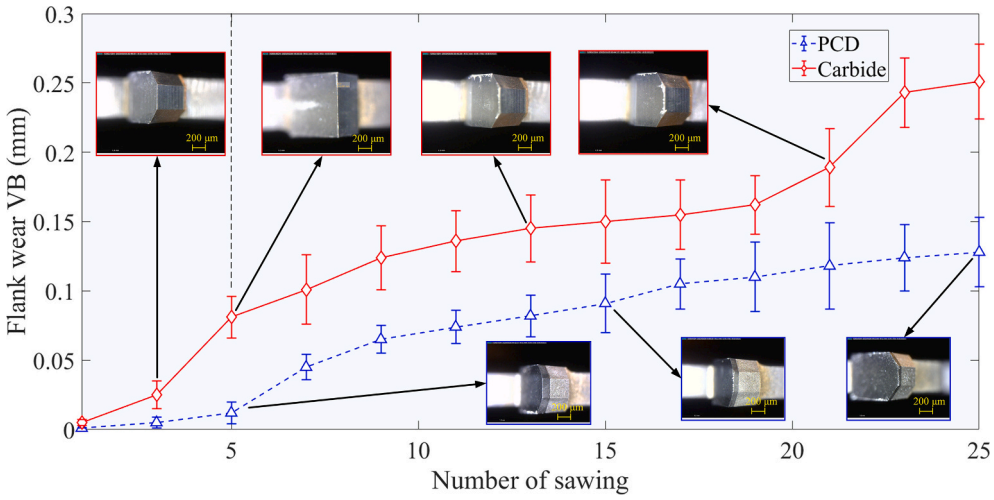

Fig. 7. Progression of the saw tooth wear average value with the number of sawing.

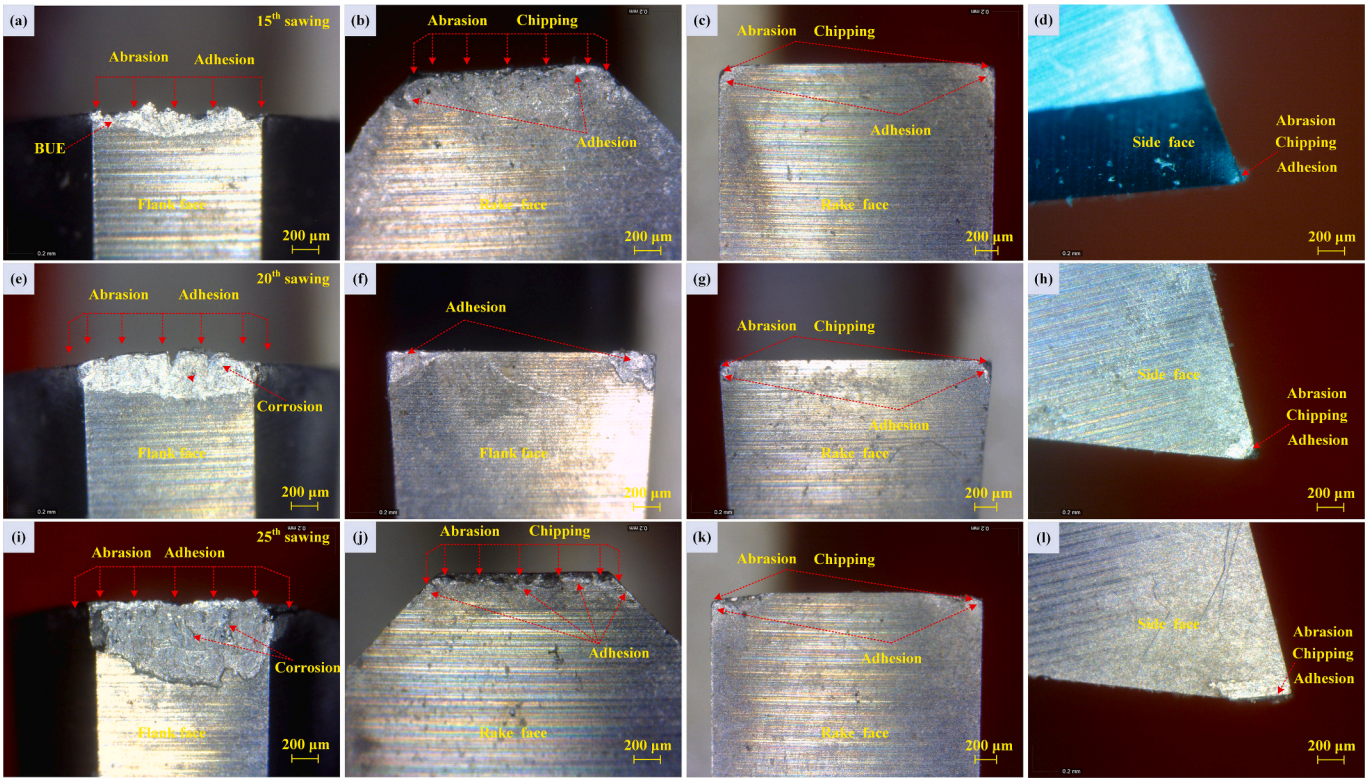

Fig. 8. Digital microscope images of the wear process of carbide tooth.

carbide teeth enter the accelerated wear phase, indicating the end of their tool life.

The wear values on the flank face of carbide and PCD teeth were measured as 0.251 mm and 0.138 mm, respectively, after 25 sawing occurrences. These measurements indicate that the carbide teeth would reach the limit of their tool life, while the PCD teeth have not yet entered the accelerated wear phase.

Fig. 8 provides a clear illustration of the varying abrasive and adhesive wear processes on different faces of the carbide teeth at the15th, 20th and 25th sawing occurrences. Fig. 8(a)-(d) show the wear state at the 15th saw, obtained from digital microscope images captured during the steady wear stage. The worn state of the saw teeth at the 20th saw is depicted in Fig. 8(e)-(h), which represent digital microscope images obtained during the accelerated wear stage. Fig. 8(i)-(l) reveal severe adhesive wear on the flank face of the carbide teeth, as well as significant abrasive and adhesive wear on the rake face. Notably, chipping and adhesive wear are prominent near the rake face of the finisher tooth, significantly impacting the sawing performance of the circular saw blade.

Fig. 9 provides a visual representation of the wear state of different faces of the PCD teeth at the 15th and 25th sawing occurrences. Fig. 9 (a)-(d) display the wear state of the saw teeth at the 15th saw, captured through digital microscope images during the steady wear stage. Minor chipping is observed at the cutting edge during this stage. The worn state of the saw teeth at the 25th saw is shown in Fig. 9(e)-(h), where the abrasive wear is more pronounced, severe adhesive wear is evident, and the chipping occurs at the cutting edge.

Fig. 10(a)–(h) depict SEM images of worn carbide and PCD teeth,

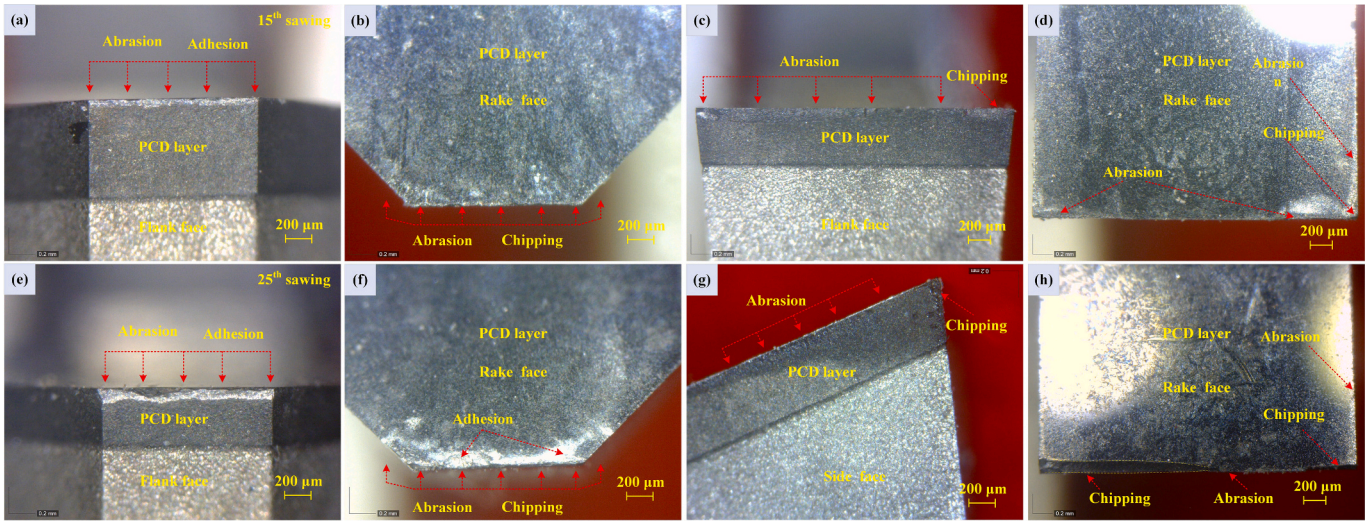

Fig. 9. Digital microscope images of the wear process of PCD tooth.

showcasing the wear achieved in the experiments. In Fig. 10(a), the micrograph illustrates the wear forms on the cutting edge and flank face of the carbide tooth. A significant accumulation of chips, forming a built-up edge (BUE), is observed on the core cutting edge. However, there is no apparent adherence on the side cutting edges, likely due to the rougher tooth type, where the side cutting edges are not extensively involved in the sawing process. Fig. 10(b) provides a local magnification of Fig. 10(a), highlighting the location of adhesive chip lamination with the carbide tooth substrate. At the end of the adhered chip, partial flaking is visible. Chip adhesion on the carbide tooth surface is demonstrated as a stack-up in Fig. 10(c), attributed to the intermittent cutting process. Fig. 10(d) shows corrosive wear on the flank face of the finisher teeth, characterized by localized corrosion near the cutting edge [10]. On the flank face, the chip corrosion is observed, which may be a result of the chemical interaction between the workpiece material and the cutting fluid or carbide.

SEM micrographs of the worn PCD saw tooth were obtained and investigated in order to further reveal the wear mechanism of the PCD saw tooth during machining of hard aluminum alloys. To facilitate comparative analysis, the PCD rougher tooth was selected as an example to demonstrate the wear mechanism, as illustrated in Fig. 10(e)–(h). In Fig. 10(e), localized chipping, characterized by fractures, can be observed in a portion of the PCD tooth. It is worth noting that while several instances of chipping wear were found, this defect is not widespread and primarily occurs due to the presence of hard particles in the hard aluminum alloys. The Al_2O_3 is formed during the sawing process, and becomes a hard gray or dark gray particle that affects saw tooth wear. This suggests that chipping wear may be attributed to the dynamic effect of hard particle formation within the chips. Fig. 10(f) provides an example of slight adhesive wear at the cutting edge of the PCD tooth. However, this adhesive wear is significantly less pronounced compared to that observed in carbide teeth. The adhesive wear is minimal and does not adversely affect the performance of the PCD tooth. To provide a more detailed analysis, Fig. 10(g) presents a local magnification of Fig. 10(e), revealing some micro-adhesion at the chipping location. The presence of micro-adhesion suggests a minor interaction between the PCD tooth and the workpiece, but the overall extent is limited. Further examination of edge wear chipping is shown in Fig. 10(h), which highlights the partial micro-adhesive wear. Although adhesion and abrasion can be observed, it remains relatively slight, indicating the robustness and durability of the PCD tooth in machining high-hardness materials. These SEM micrographs provide valuable insights into the wear characteristics of the PCD tooth, emphasizing its potential for prolonged tool life and suitability for machining high-hardness materials such as the 7075 aluminum alloys.

To gain a comprehensive understanding of the adhesive wear and diffusive wear of carbide teeth, Energy Dispersive Spectroscopy (EDS) analysis was conducted. Fig. 11–13 illustrate the actual contact area between the saw tooth and the workpiece interface, revealing the presence of bulges. At elevated temperatures and under high-stress conditions, plastic deformation and adhesion take place at the interface, resulting in the formation of micro-welds [20]. Due to the relative motion between the saw teeth and the workpiece, shearing can occur at the original interface or along paths above or below it, leading to adhesive wear. Shearing can also occur in vulnerable areas of the harder material, facilitated by a few bulges present in the harder material. As illustrated in Fig. 11, the partial normal force (N_{VB}) is generated along the saw tooth-workpiece interface by the micro-welds. Once abrasive wear occurs, adhesive wear enlarges the sawing force, which in turn aggravates the wear. Referring to [20], the total tool adhesive wear volume loss $\widehat{V}_{wear-adhesion}$ can be denoted as:

$$\widehat{V}_{wear-adhesion} = K_{adhesion} e^{aT} v_s b \bar{\sigma} \Delta t \tag{1}$$

where a and b are hardness constants. $K_{adhesion} = p_0 K_0 (1 - p_{adhesion}\%)/b$, is the coefficient of adhesive wear. For the same combination of the saw tooth and the workpiece, $K_{adhesion}$ is treated as a constant. T is temperature. p_0 is the probability to form a sizable wear particle from the harder material. K_0 is a constant. $p_{adhesion}\%$ is the percentage of the total normal force supported by abrasive particles. v_s is the sawing rotational speed and v_f is the feed rate. $\bar{\sigma}$is average normal stress, and $\Delta t$is time interval. The wear volume loss due to adhesion does not determine the length VB of the flank face wear, but rather the sliding distance $v_s \Delta t$ [36].

The EDS analysis provides valuable insights into the wear mechanisms of the saw teeth, shedding light on the adhesive wear and diffusive wear phenomena. By understanding these mechanisms, further improvements can be made to optimize the design and performance of saw teeth in machining applications. Carbide particles exhibit chemical stability when in contact with the workpiece. However, during high-speed sawing processes, the worn carbide teeth and workpiece experience significant friction, leading to the generation of high temperatures and high stresses. These conditions can cause elements such as Al or Mg in the workpiece to become relatively unstable, resulting in chemical reactions. Specifically, the formation of Al_2O_3 and MgO can occur during sawing process, as represented by Eqs. (2) and (3), resulting in the formation of partially hard particles. Fig. 12(a) illustrates the presence of adhesive wear on the flank face, accompanied by slight element

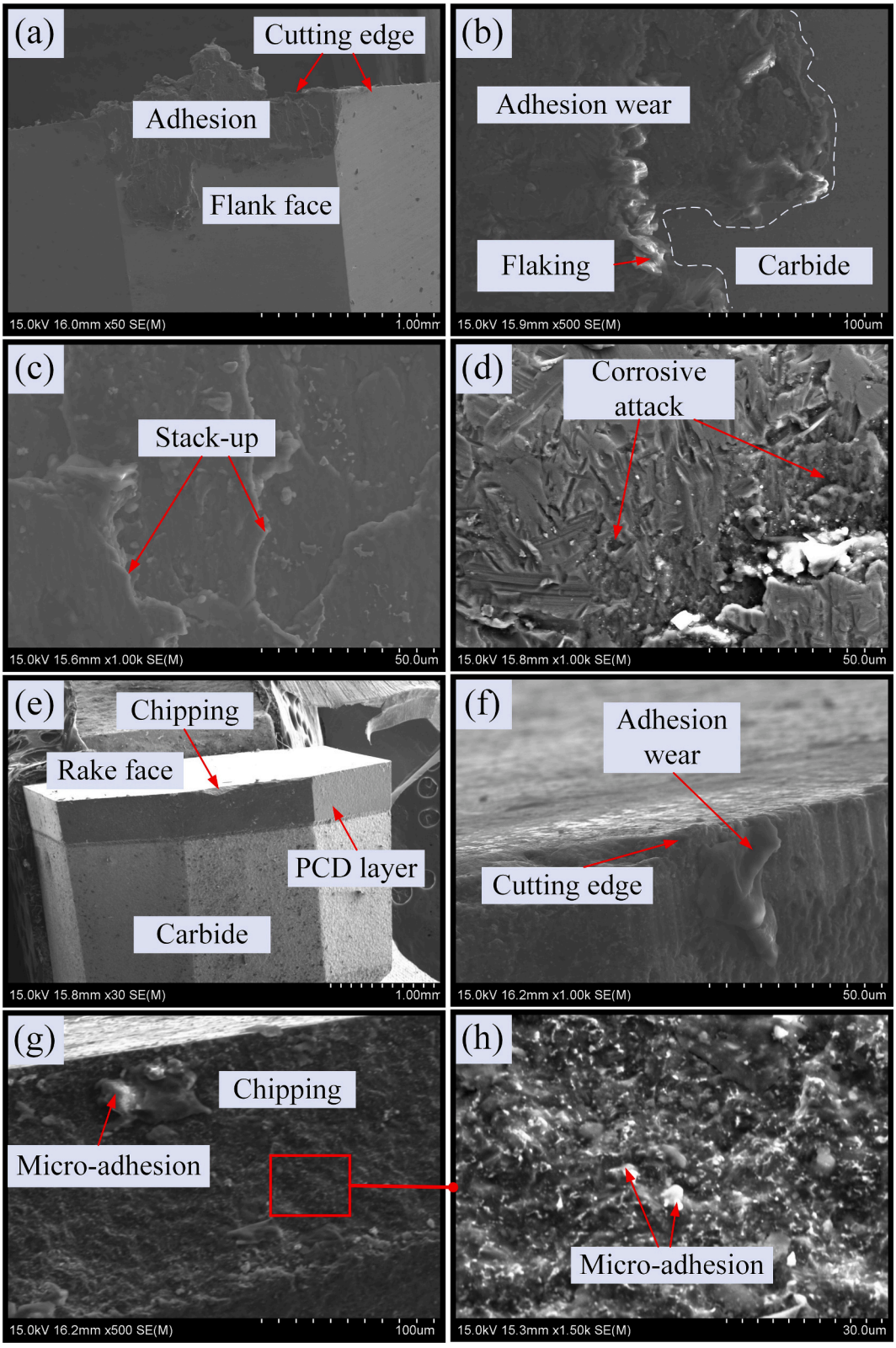

Fig. 10. SEM micrographs of worn (a)-(d) carbide and (e)-(h) PCD teeth.

diffusion in the unadhered area. Upon adhesion to the flank face, the carbide tooth is observed to be almost completely covered, as demonstrated by the line scan spectrum distribution of tungsten elements in Fig. 12(b). These observations suggest that the chemical activity between the worn carbide teeth and the workpiece, combined with the high temperatures and stresses involved, contributes to the formation of Al_2O_3 and MgO compounds. The adhesive wear and element diffusion further highlight the complex interplay between the saw teeth and the workpiece during the sawing process.

$$4Al + 3O_2 = 2Al_2O_3 \quad (2)$$

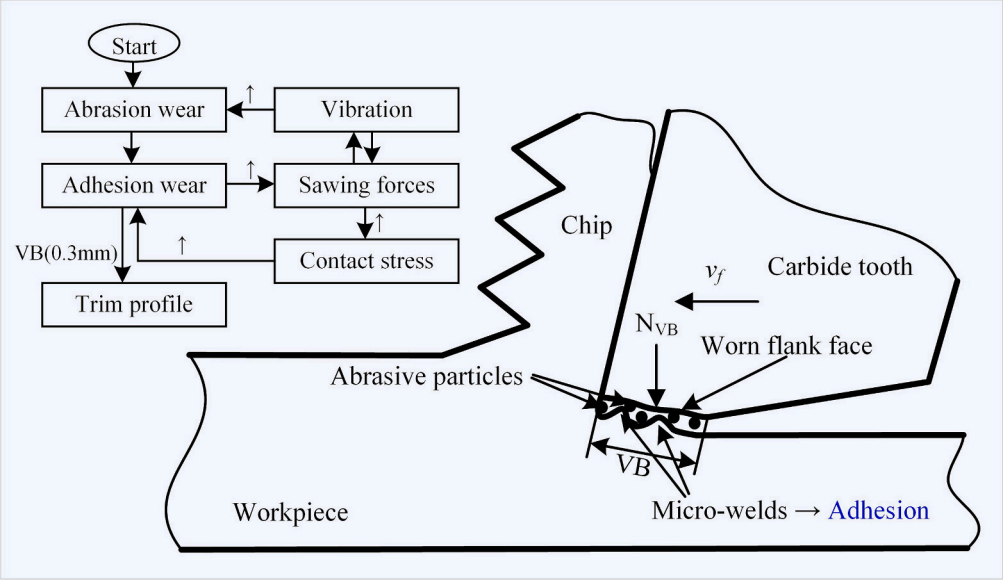

Fig. 11. Schematic diagram of the tooth-workpiece interface.

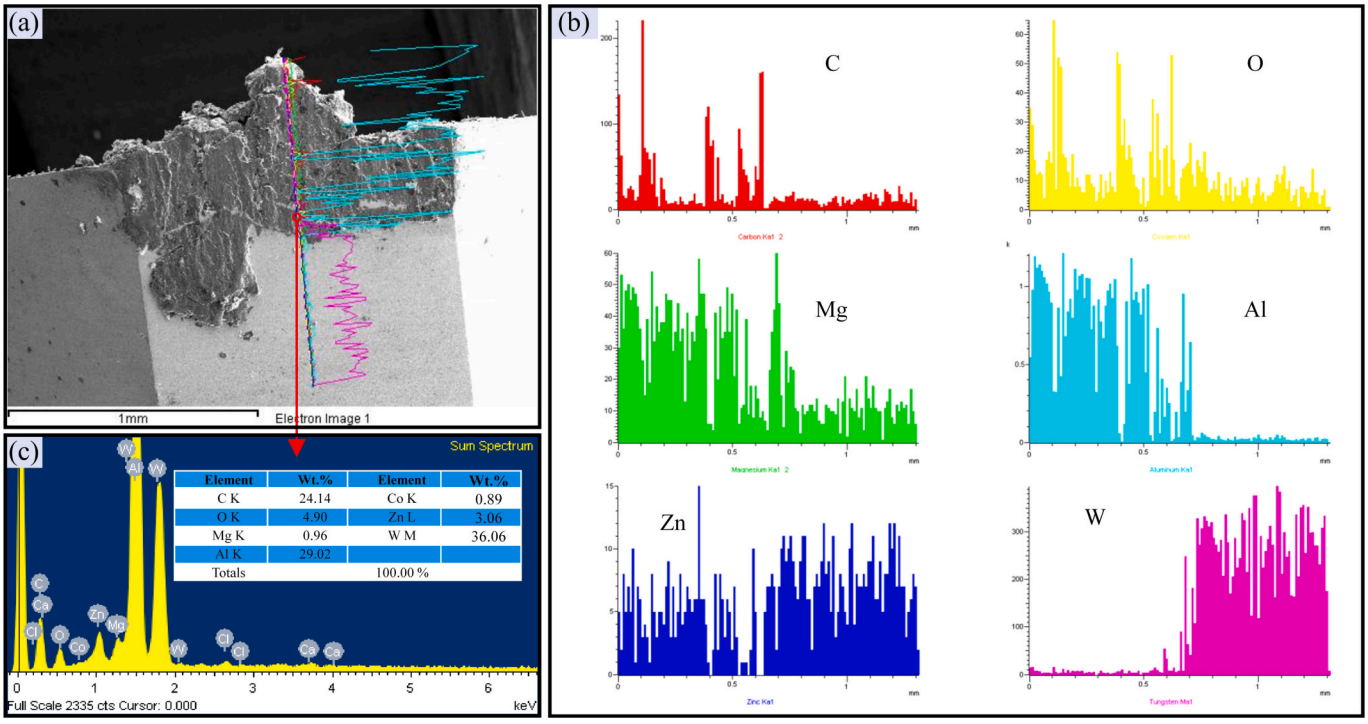

Fig. 12. SEM photograph and EDS spectrum analysis by line scan for worn carbide tooth.

$$2Mg + O_2 = 2MgO \quad (3)$$

Fig. 13(a) presents a 3D image of a section of the carbide tooth, providing a detailed view of its surface characteristics. The flank face of the saw tooth, exhibiting severe adhesive wear, is depicted in Fig. 13(b). The extent of adhesion on the saw tooth is quantified in terms of height, as shown in Fig. 13(c). Notably, Fig. 13(d) visualizes that the adhesive length exceeds 800 μm, while the adhesive thickness is nearly 40 μm. The adhesive wear prominently covers the cutting edge on the flank face, and its substantial height significantly increases the removal of the saw tooth/workpiece contact area. Consequently, this reinforces the likelihood of saw tooth wear and contributes to the generation of larger sawing forces. Moreover, the presence of this adhesion layer during the sawing process can result in repeated mechanical and thermal shocks exerted on the workpiece. The results suggest that the severe adhesive wear observed on the flank face of the carbide tooth has a substantial impact on the overall performance and longevity of the circular saw blade. Understanding and mitigating such adhesive wear are crucial for improving the efficiency and durability of circular saw blades.

The assessment of sawing performance for saw teeth primarily focuses on the type of wear observed on the cutting edge during the sawing of hard aluminum alloys. SEM images depicting the dominant wear mechanisms on the cutting edge are presented in Fig. 14(a)-(f). On the carbide finisher teeth, Fig. 14(a) reveals noticeable adhesive wear,

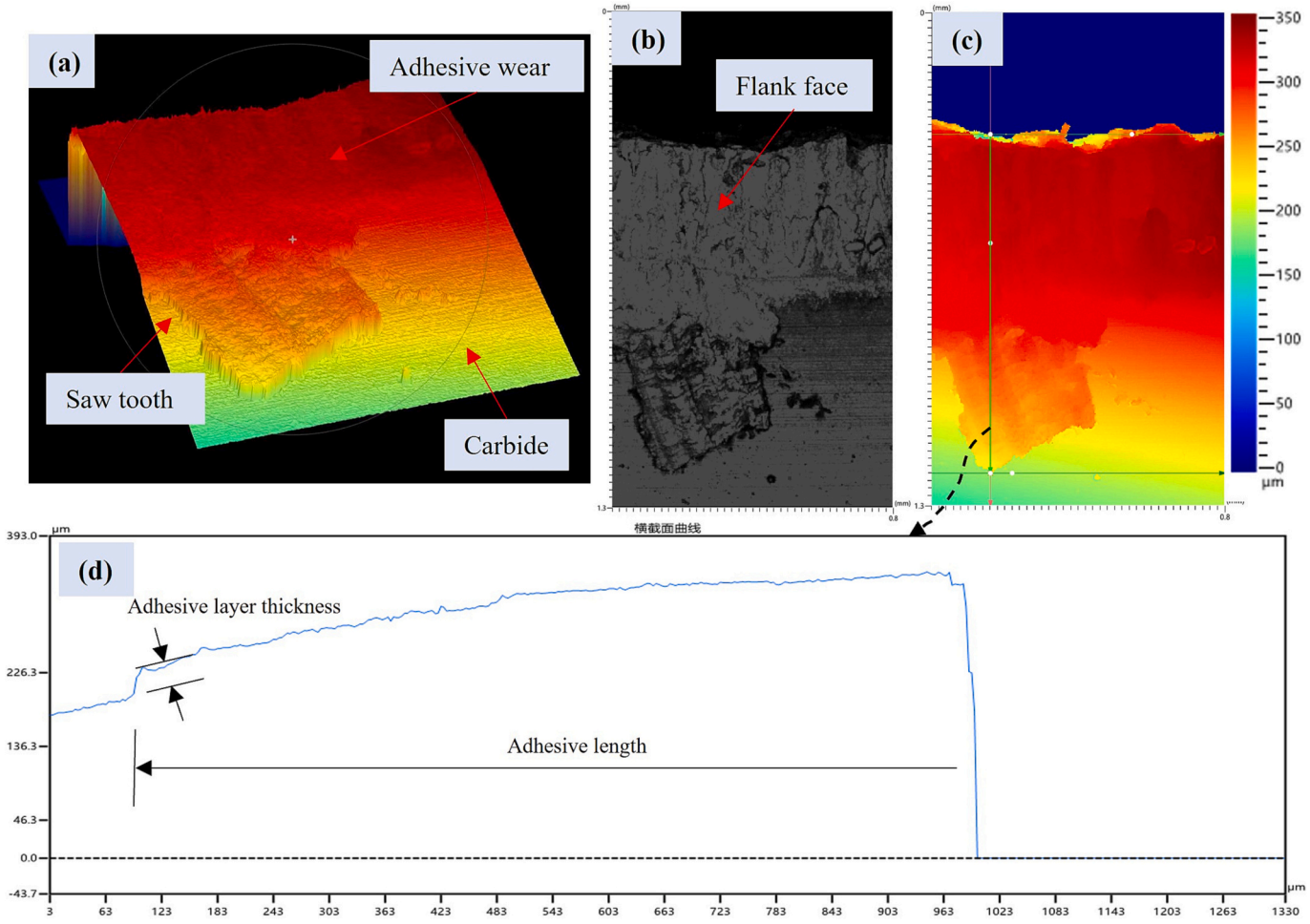

Fig. 13. Observation of adhesive wear for worn carbide tooth.

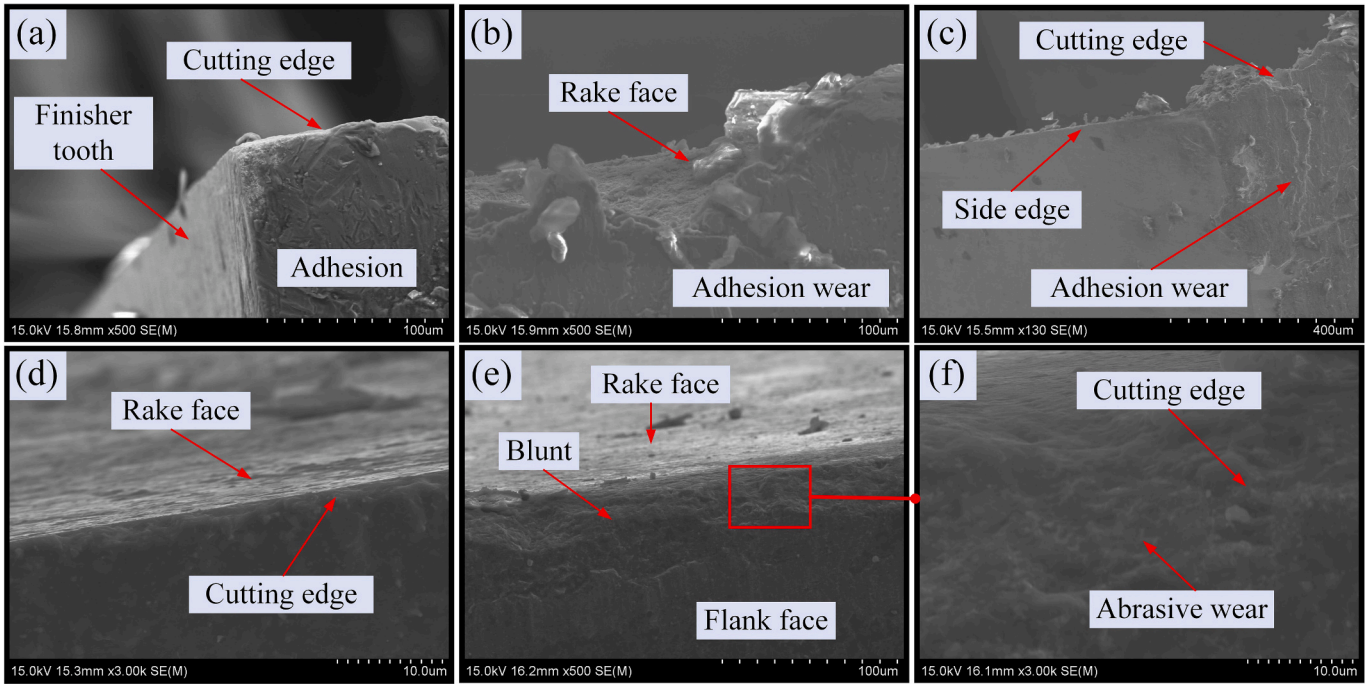

Fig. 14. SEM photographs of dominant wear mechanisms on the cutting edge of (a)-(c): carbide and (d)-(f): PCD teeth.

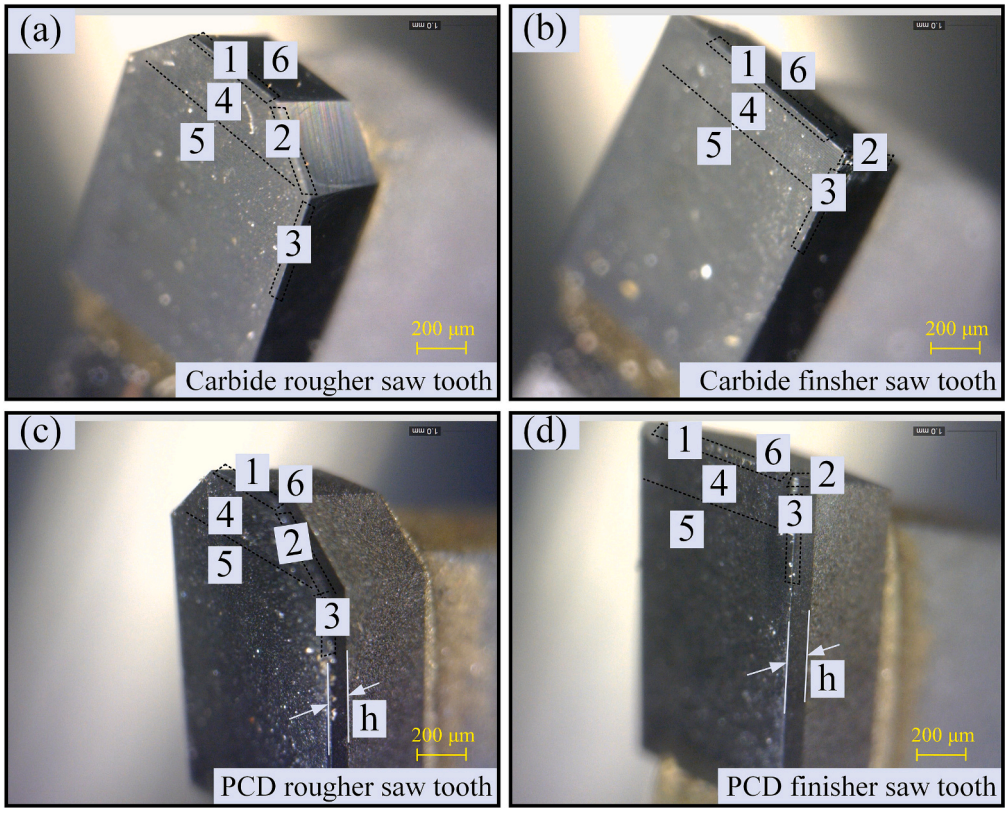

Fig. 15. Definition of wear zones for (a), (b) carbide and (c), (d) PCD teeth: (1) cutting edge; (2) side edge corner; (3) cutting sides; (4) tooth bite surface; (5) rake face; (6) flank face.

Table 2
Wear mechanisms of carbide rougher tooth.

Mark	Zones	Adhesion	Abrasion	Chipping	Corrosion	Oxidation	Cracking
(1)	Cutting edge	•	•	•		•	•
(2)	Side edge corner	•	•	•			•
(3)	Cutting sides	•	•			•	
(4)	Tooth bite surface	•	•		•	•	
(5)	Rake surface	•	•				
(6)	Flank surface	•	•		•	•	

accompanied by corrosive wear in the adhesive zones, resulting in blunting of the finisher teeth. Fig. 14(b) illustrates severe adhesive wear occurring on the cutting edge and the rake face of the rougher tooth, significantly impairing the sawing performance. However, the adhesive wear is not observed on the side edges of the rougher teeth due to their limited exposure time to the sawing process and the small chip thickness, as mentioned earlier (Fig. 14(c)).

Fig. 14(d)-(f) display SEM images of the dominant wear morphologies of the PCD teeth. As sawing time increases, the cutting edges of the PCD teeth degrade. Slight adhesive wear is observed on the rake face and cutting edge (Fig. 14(d)), while abrasive wear is detected on the cutting edges, as shown in Fig. 14(f). Additionally, minor chipping is identified in one of the PCD teeth, mainly occurring in the middle of the cutting edge (Fig. 14(e)). Chipping is observed during the stable sawing phase, where continuous degradation of the cutting edge, primarily due to abrasive wear, potentially accompanied by tribochemical wear.

Multiple wear mechanisms come into action, including abrasion, friction chemistry, chipping, delamination, and cracking during the sawing process of hard aluminum alloys [37,38]. These wear mechanisms can be observed on the worn carbide or PCD teeth, although two or three mechanisms may predominate. In this work, the wear mechanisms present in each wear zone of the saw teeth are characterized. Fig. 15 and Tables 2–5 illustrate the types of wear mechanisms identified in each specific wear zone. A detailed description is provided below.

Table 3
Wear mechanisms of carbide finisher tooth.

Mark	Zones	Adhesion	Abrasion	Chipping	Corrosion	Oxidation	Cracking
(1)	Cutting edge	•	•	•		•	•
(2)	Side edge corner	•	•				
(3)	Cutting sides	•	•			•	
(4)	Tooth bite surface	•	•		•	•	
(5)	Rake surface		•				
(6)	Flank surface	•	•		•	•	

Table 4
Wear mechanisms of PCD rougher tooth.

Mark	Zones	Adhesion	Abrasion	Chipping	Corrosion	Oxidation	Cracking
(1)	Cutting edge	•	•	•		•	•
(2)	Side edge corner	•	•	•		•	
(3)	Cutting sides	•	•			•	
(4)	Tooth bite surface		•				
(5)	Rake surface		•				
(6)	Flank surface		•				

Table 5
Wear mechanisms of PCD finisher tooth.

Mark	Zones	Adhesion	Abrasion	Chipping	Corrosion	Oxidation	Cracking
(1)	Cutting edge	•	•	•		•	•
(2)	Side edge corner		•				
(3)	Cutting sides	•	•			•	
(4)	Tooth bite surface		•				
(5)	Rake surface		•				
(6)	Flank surface		•				

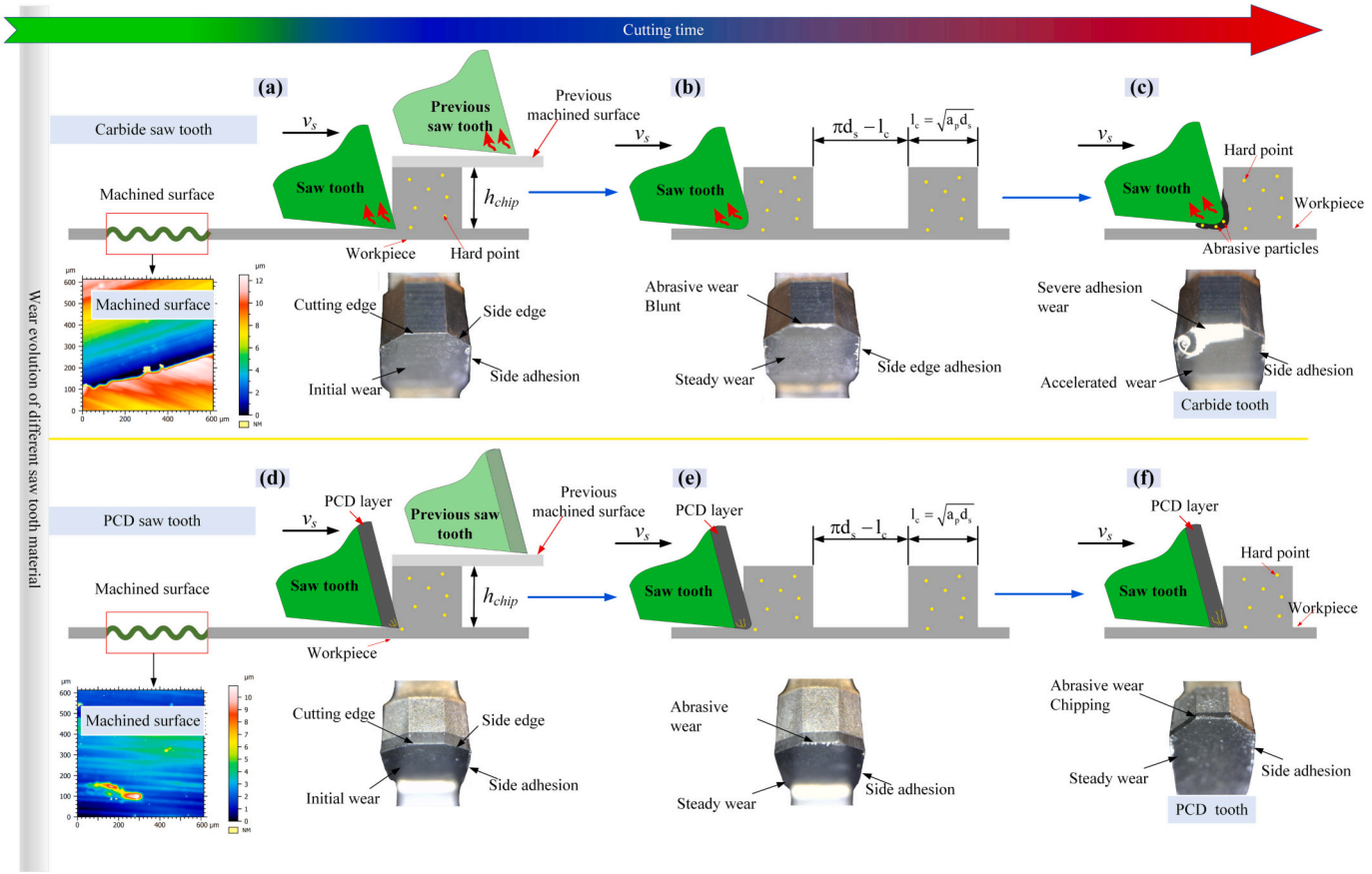

Fig. 16. Schematic of wear evolution of carbide and PCD teeth.

As depicted in Fig. 8–14, the primary wear mechanisms observed in the worn carbide teeth are abrasion and adhesion. Abrasive wear refers to the gradual removal of material from the tooth surface due to mechanical interactions with the workpiece, while adhesive wear involves the formation of adhesion layers on the tooth surface as a result of high temperature and stress. These wear mechanisms are prominently exhibited in the carbide teeth.

The predominant wear mechanisms observed in the worn PCD teeth are abrasive and chipping [13]. Abrasive wear occurs due to the sawing action of hard particles or chips, resulting in the gradual degradation of the cutting edges. Chipping wear, characterized by localized fracture and chip formation, is also observed on the PCD teeth. These wear mechanisms play a significant role in determining the performance and lifespan of the PCD teeth. By analyzing and understanding the specific wear mechanisms present in each wear zone of the saw teeth, valuable insights can be gained for optimizing the design and material selection of sawing tools, thereby improving their overall performance in sawing hard aluminum alloys.

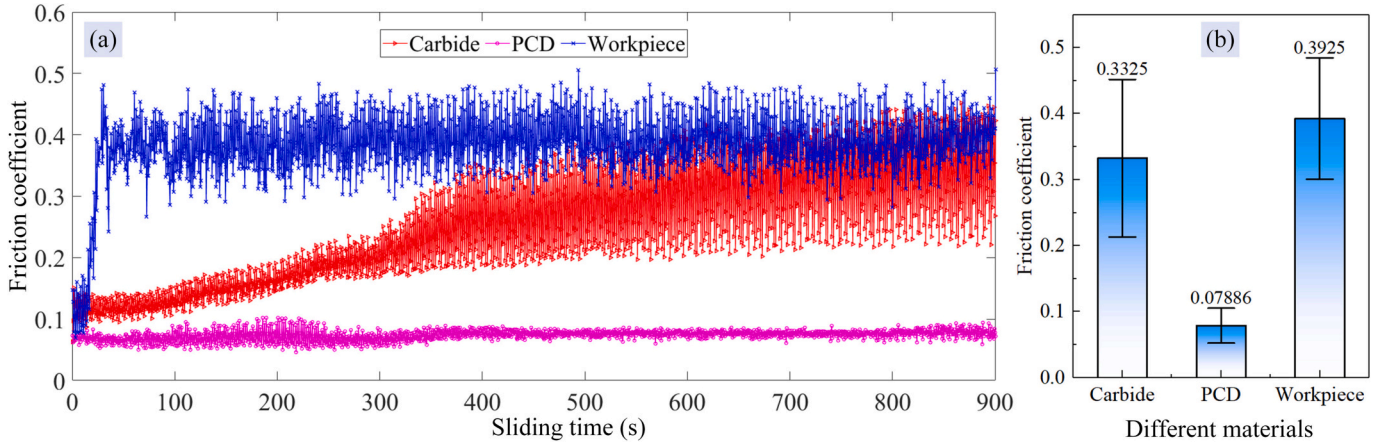

Fig. 17. (a) Dynamic friction coefficients. (b) comparison of coefficients.

3.3. Analysis of wear evolution of saw teeth

An in-depth understanding of the wear behavior of the saw teeth is the key to analyzing the different wear stages in sawing hard aluminum alloys. In Section 3.2, the wear behavior of different saw tooth materials is characterized separately. A comprehensive model depicting the wear evolution of different saw tooth materials, specifically focusing on the wear process of the rougher teeth, is presented in Fig. 16.

Fig. 16(a)-(c) present the wear evolution of the carbide teeth, which can be divided into the following three main stages: initial wear, steady wear and accelerated wear. Normally, before sawing, it is necessary to resharpen the carbide teeth to ensure a sharp cutting edge in Fig. 16(a). During the initial wear stage, the cutting edge remains sharp, resulting in light and fast cutting. After a few sawing passes, the saw teeth gradually reach a stable wear state, as shown in Fig. 16(b). In this stage, the cutting edge becomes dull, adhesive wear becomes apparent, and a significant amount of cutting heat is transferred to the saw tooth, leading to thermal adhesion. As illustrated in Fig. 16(c), the accelerated wear stage is reached, characterized by severe adhesion, corrosion in the adhesion region, and thermal cracking.

The wear evolution of the PCD teeth is illustrated in Fig. 16(d)-(f). The inclusion of a PCD layer significantly extends the lifespan of the tool, reaching approximately 10 times that of carbide teeth. In the initial stage of wear, there is a slight occurrence of abrasive wear caused by the PCD layer's low friction coefficient and excellent thermal conductivity. This attribute results in lower cutting heat generated compared to carbide teeth. As the saw time increases, the PCD layer collides reciprocally with the hard particles present in the hard aluminum alloy, leading to abrasive wear of the PCD teeth. However, when the carbide teeth were in the accelerated wear phase, the PCD teeth experienced only minor

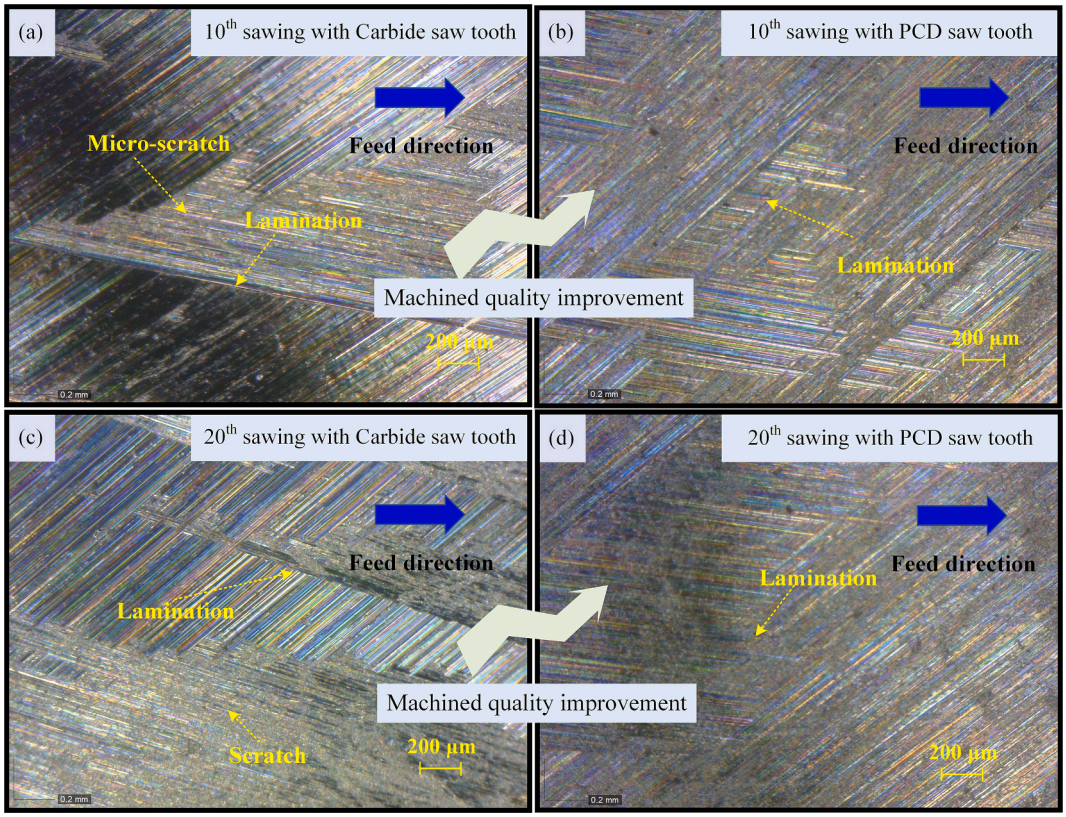

Fig. 18. Qualities of the machined surfaces with carbide and PCD circular saw blades (the 10th and 20th sawing).

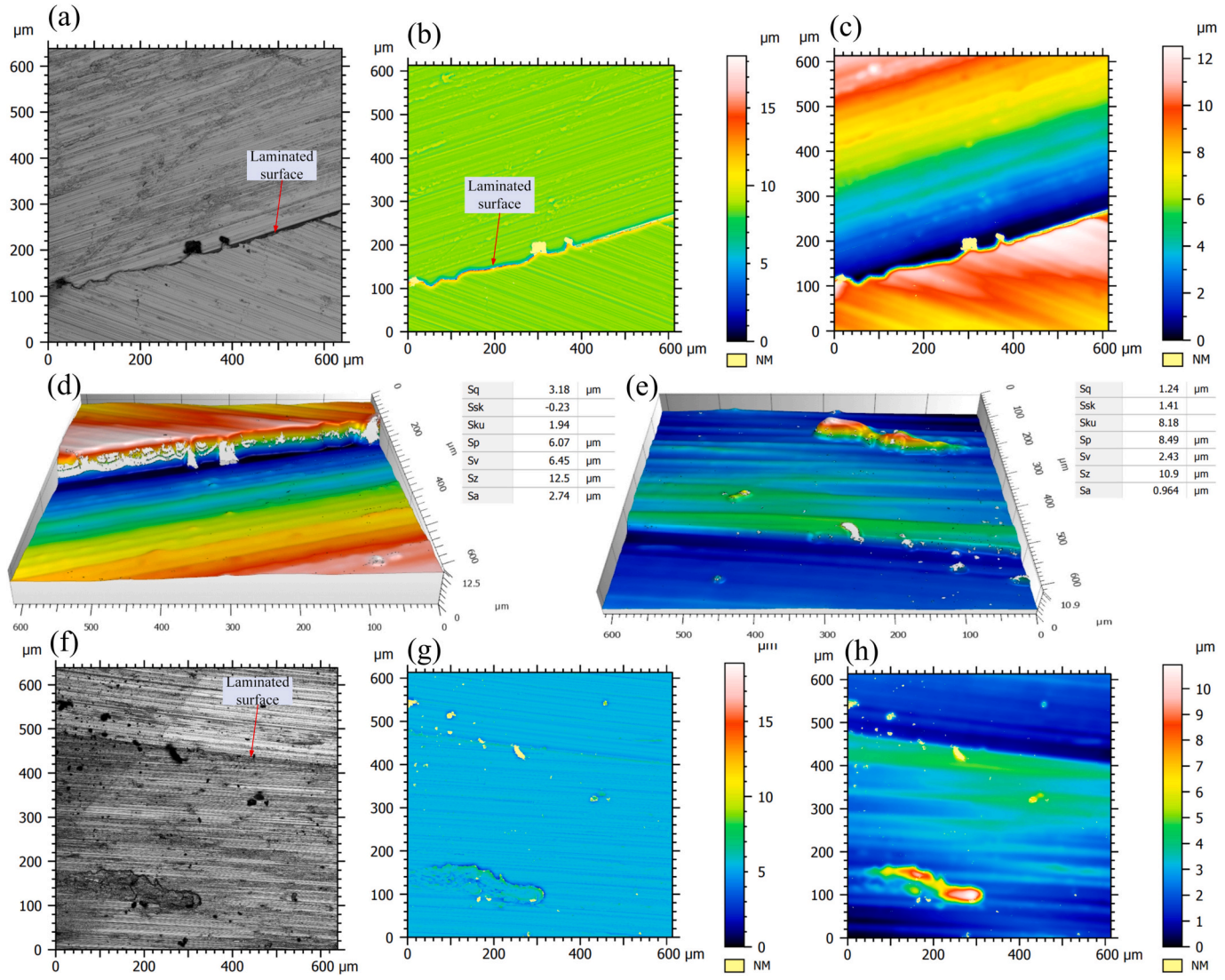

Fig. 19. Scanning photographs of machined surfaces with (a)-(d) carbide and (e)-(h) PCD circular saw blades (the 10th sawing).

chipping, as depicted in Fig. 16(f). This outcome is primarily due to the exceptional performance of PCD in aluminum alloy sawing. It is worth noting that the wear process described above also applies to the finisher teeth.

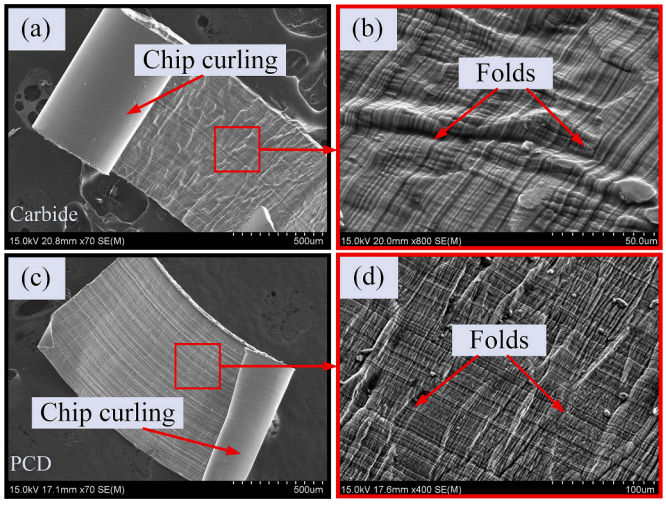

Fig. 20. SEM photographs of chip morphology with carbide and PCD circular saw blades (the 10th sawing).

The tribological wear performance of carbide material, PCD material and workpiece material were assessed under room temperature and dry friction conditions by sliding friction and wear tests, as seen in Fig. 17. Fig. 17(a) illustrates the dynamic variations of the friction coefficient of the three materials with slipping time. The PCD sample is relatively stable and does not change significantly, while the carbide sample gradually stabilizes with the growth of slipping time, and the friction coefficient of the workpiece sample is larger and stabilizes to about 0.4. The friction coefficient of the PCD sample is approximately 0.078, which provides excellent thermal stability and wear resistance, and can meet the sawing requirements of the workpiece. The friction coefficient of the carbide sample is far greater than that of the PCD sample and is relatively unstable, which explains the severe adhesive wear of carbide teeth during sawing of hard aluminum alloys. At dry friction conditions, the friction coefficients of the carbide and workpiece samples were unstable and intensely fluctuated during the whole sliding time of 900 s. In contrast, the friction coefficient of the PCD sample is low and stable during the subsequent sliding time, which has a promising friction-relieving role. This also means that the wear evolution life of PCD teeth is considerably longer than that of carbide teeth.

To further understand the machining performance of carbide and PCD circular saw blades, Machined surface qualities were obtained by digital microscopy and confocal microscopy, as shown in Fig. 18 and 19. Fig. 18 shows the qualities of the machined surfaces with carbide and PCD circular saw blades at different sawing times. The appearance of the laminated surface can be clearly seen in Fig. 18(a), which is consistent with the analysis in Fig. 4(c). It can be concluded that the use of PCD teeth is superior to carbide teeth. Fig. 19(a)-(d) depict the surface integrity of machining with carbide teeth. The surface integrity of the machining with PCD teeth is presented in Fig. 19(e)-(h). As indicated in Fig. 19(c), the surface morphology using the carbide tooth is inferior to that of the PCD tooth (Fig. 19(h)). Fig. 19(d) shows the surface roughness of 12.5 μm with carbide teeth, while the machined surface roughness with PCD teeth is 10.9 μm, thus it can be derived that the sawing performance of PCD teeth is preferable to carbide teeth.

Fig. 20 reveals a noteworthy observation regarding the chip morphology of carbide and PCD teeth. In Fig. 20(a), it can be observed that both types of teeth produce curled chips. The chips exhibit a folded structure, forming serrated chips [39,40]. A comparison between Fig. 20 (b) and (d) demonstrate a similarity in the surface morphology of the chips, albeit with the chips from the PCD teeth appearing slightly smoother. It is worth noting that the chips generated by the two types of teeth exhibit a considerable resemblance, and the observed differences in the chips do not appear to possess significant meaning.

4. Conclusion

In this research, a comprehensive investigation was conducted to systematically study the saw tooth wear. The wear morphology of carbide and PCD teeth was meticulously monitored in real-time as the number of saw times increased. Furthermore, the wear mechanism of the saw teeth was extensively explored using SEM, developing a detailed schematic representation of the wear evolution of saw teeth. The significant contributions of this study can be summarized as follows:

(1) The metal sawing process involves intricate frictional, physical and chemical behaviors. The wear mechanism of carbide teeth is primarily abrasion, adhesion and corrosion, while the wear mechanism of PCD teeth is mainly abrasion and minor chipping damage.
(2) The zones of carbide and PCD teeth were categorized based on the specific forms of wear in different positions. The cutting edge of carbide teeth primarily experiences abrasion and adhesion, while the flank faces primarily undergo adhesion and diffusion. In contrast, the main wear form observed on the cutting edge of PCD teeth is abrasive and chipping. From the perspective of the flank face wear, the lifespan of PCD teeth far exceeds that of carbide teeth.
(3) An exhaustive schematic representation of the wear evolution of the carbide and PCD teeth are given. The primary cause of wear in carbide teeth is cutting heat, whereas the presence of hard particles in the machined workpiece is the dominant factor contributing to wear in PCD teeth by SEM and EDS analysis. These findings align with the actual wear phenomena observed during the experiments.
(4) The machined surface achieved with PCD teeth exhibits superior quality compared to that obtained with carbide teeth. Additionally, the appearance of the chips produced by both materials' saw teeth is found to be similar.

Disclosure statement

No potential conflict of interest was reported by the authors.

CRediT authorship contribution statement

Jinyou Kang: Conceptualization, Methodology, Investigation, Writing – original draft. **Jinsheng Zhang:** Writing – review & editing, Supervision, Funding acquisition. **Kaida Wang:** Methodology, Validation. **Dongfang Zhang:** Supervision, Formal analysis. **Tianyu Bai:** Methodology, Investigation. **Heng Zhang:** Validation, Writing – review & editing. **Weiye Song:** Supervision, Writing – review & editing.

Declaration of Competing Interest

We declare that we do not have any commercial or associative interest that represents a conflict of interest in connection with the work submitted.

Data availability

No data was used for the research described in the article.

Acknowledgments

This research was supported by the Key Research and Development Project of Rizhao [NO. 2021ZDYF010109], the Rizhao Natural Science Foundation Project [NO. RZ2021ZR35] and the Shandong Provincial Natural Science Foundation [ZR2023QE162].

References

[1] P. Zhang, L. Zeng, X. Mi, Y. Lu, S. Luo, W. Zhai, Comparative study on the fretting wear property of 7075 aluminum alloys under lubricated and dry conditions, Wear 474 (2021), 203760, https://doi.org/10.1016/j.wear.2021.203760.
[2] P. Zhang, X. Zhang, X. Cao, X. Yu, Y. Wang, Analysis on the tool wear behavior of 7050 t7451 aluminum alloy under ultrasonic elliptical vibration cutting, Wear 466 (2021), 203538, https://doi.org/10.1016/j.wear.2020.203538.
[3] V. Calatoru, M. Balazinski, J. Mayer, H. Paris, G. L'Esp'erance, Diffusion wear mechanism during high speed machining of 7475-t7351 aluminum alloy with carbide end mills, Wear 265 (11−12) (2008) 1793–1800, https://doi.org/10.1016/j.wear.2008.04.052.
[4] S. Li, C. Wang, L. Zheng, Y. Wang, X. Xu, F. Ding, Dynamic stability of cemented carbide cir cular saw blades for woodcutting, J. Mater. Process. Technol. 238 (2016) 108–123, https://doi.org/10.1016/j.jmatprotec.2016.07.018.
[5] V. Nasir, M. Kooshkbaghi, J. Cool, F. Sassani, Cutting tool temperature monitoring in circular sawing: measurement and multi-sensor feature fusion-based prediction, Int. J. Adv. Manuf. Technol. 112 (2021) 2413–2424, https://doi.org/10.1007/s00170-020-06473-6.
[6] C. Kalyan, G. Samuel, Cutting mode analysis in high speed finish turning of almgsi alloy us ing edge chamfered pcd tools, J. Mater. Process. Technol. 216 (2015) 146–159, https://doi.org/10.1016/j.jmatprotec.2014.09.003.
[7] V. Calatoru, M. Balazinski, J. Mayer, H. Paris, G. L'Esp'erance, Diffusion wear mechanism during high speed machining of 7475-t7351 aluminum alloy with carbide end mills, Wear 265 (11–12) (2008) 1793–1800, https://doi.org/10.1007/s40684-022-00416-0.
[8] J. Nordström, J. Bergström, Wear testing of saw teeth in timber cutting, Wear 250 (1−12) (2001) 19–27, https://doi.org/10.1016/S0043-1648(01)00625-1.
[9] Y. Meng, J. Wei, J. Wei, H. Chen, Y. Cui, An ansys/ls-dyna simulation and experimental study of circular saw blade cutting system of mulberry cutting machine, Comput. Electron. Agric. 157 (2019) 38–48, https://doi.org/10.1016/j.compag.2018.12.034.
[10] D. Lewis, S. Bradbury, M. Sarwar, Analysis of the wear and failure mechanisms that develop in high speed steel circular saw blades when machining nickel-based alloys, Wear 197 (1–2) (1996) 74–81, https://doi.org/10.1016/0043-1648(95)06834-1.
[11] B. Wang, Z. Liu, Cutting performance of solid ceramic end milling tools in machining hardened aisi h13 steel, Int. J. Refract. Met. Hard Mater. 55 (2016) 24–32, https://doi.org/10.1016/j.ijrmhm.2015.11.004.
[12] X. Wang, V.L. Popov, Z. Yu, Y. Li, J. Xu, Q. Li, H. Yu, Evaluation of the cutting performance of micro-groove-textured pcd tool on sicp/al composites, Ceram. Int. 48 (21) (2022) 32389–32398, https://doi.org/10.1016/j.ceramint.2022.07.182.
[13] J. Arsecularatne, L. Zhang, C. Montross, Wear and tool life of tungsten carbide, pcbn and pcd cutting tools, Int. J. Mach. Tools Manuf. 46 (5) (2006) 482–491, https://doi.org/10.1016/j.ijmachtools.2005.07.015.
[14] R. Lindvall, F. Lenrick, H. Persson, R. M'Saoubi, J.-E. Ståhl, V. Bushlya, Performance and wear mechanisms of pcd and pcbn cutting tools during machining titanium alloy ti6al4v, Wear 454 (2020), 203329, https://doi.org/10.1016/j.wear.2020.203329.
[15] G. List, M. Nouari, D. G'ehin, S. Gomez, J.-P. Manaud, Y. Le Petitcorps, F. Girot, Wear behaviour of cemented carbide tools in dry machining of aluminium alloy,

Wear 259 (7–12) (2005) 1177–1189, https://doi.org/10.1016/j.wear.2005.02.056.
[16] R. Lindvall, F. Lenrick, R. M'Saoubi, J.-E. Ståhl, V. Bushlya, Performance and wear mechanisms of uncoated cemented carbide cutting tools in ti6al4v machining, Wear 477 (2021), 203824, https://doi.org/10.1016/j.wear.2021.203824.
[17] Z. Zhang, Q. Zhang, W. Wang, N. Yu, W. Ding, J. Xu, Wear evolution of microstructured diamond grains in wc/co cemented carbide single grain scratching, Wear 488 (2022), 204142, https://doi.org/10.1016/j.wear.2021.204142.
[18] J. Liang, H. Gao, S. Xiang, L. Chen, Z. You, Y. Lei, Research on tool wear morphology and mechanism during turning nickel-based alloy gh4169 with pvd-tialn coated carbide tool, Wear 508 (2022), 204468, https://doi.org/10.1016/j.wear.2022.204468.
[19] J. Zhao, Z. Liu, B. Wang, J. Hu, Y. Wan, Tool coating effects on cutting temperature during metal cutting processes: comprehensive review and future research directions, Mech. Syst. Signal Process. 150 (2021), 107302, https://doi.org/10.1016/j.ymssp.2020.107302.
[20] Y. Huang, S.Y. Liang, Modeling of cbn tool flank wear progression in finish hard turning, J. Manuf. Sci. Eng. 126 (1) (2004) 98–106, https://doi.org/10.1115/1.1644543.
[21] P. Masek, J. Maly, P. Zeman, P. Heinrich, N.T. Alagan, Turning of titanium alloy with pcd tool and high-pressure cooling, J. Manuf. Process. 84 (2022) 871–885, https://doi.org/10.1016/j.jmapro.2022.10.034.
[22] D. Boing, R.B. Schroeter, A.J. de Oliveira, Three-dimensional wear parameters and wear mechanisms in turning hardened steels with pcbn tools, Wear 398 (2018) 69–78, https://doi.org/10.1016/j.wear.2017.11.017.
[23] D.J. Schrock, D. Kang, T.R. Bieler, P. Kwon, Phase dependent tool wear in turning ti-6al-4v using polycrystalline diamond and carbide inserts, J. Manuf. Sci. Eng. 136 (4) (2023), https://doi.org/10.1115/1.4027674.
[24] C.E. Ventura, F.C. Magalhães, A.M. Abrão, B. Denkena, B. Breidenstein, Performance evaluation of the edge preparation of tungsten carbide inserts applied to hard turning, Int. J. Adv. Manuf. Technol. 112 (2021) 3515–3527, https://doi.org/10.1007/s00170-020-06585-z.
[25] G. Li, S. Yi, C. Wen, S. Ding, Wear mechanism and modeling of tribological behavior of polycrys talline diamond tools when cutting ti6al4v, J. Manuf. Sci. Eng. 140 (12) (2023), https://doi.org/10.1115/1.4041327.
[26] X. Li, X. Liu, C. Yue, S.Y. Liang, L. Wang, Systematic review on tool breakage monitoring tech niques in machining operations, Int. J. Mach. Tools Manuf. (2022), 103882, https://doi.org/10.1016/j.ijmachtools.2022.103882.
[27] J. Sheikh-Ahmad, J. Bailey, The wear characteristics of some cemented tungsten carbides in machining particleboard, Wear 225 (1999) 256–266, https://doi.org/10.1016/S0043-1648(98)00361-5.
[28] Y. Lu, J. Deng, Q. Sun, D. Ge, J. Wu, Z. Zhang, Effect of micro textures on the cutting performance of circular saw blade, Int. J. Adv. Manuf. Technol. 115 (9–10) (2021) 2889–2903, https://doi.org/10.1007/s00170-021-07348-0.
[29] D. Lewis, S. Bradbury, M. Sarwar, The effect of substrate surface preparation on the wear and failure modes of tin coated high speed steel circular saw blades, Wear 197 (1–2) (1996) 82–88, https://doi.org/10.1016/0043-1648(95)06835-X.
[30] R. Licow, D. Chuchala, M. Deja, K.A. Orlowski, P. Taube, Effect of pine impregnation and feed speed on sound level and cutting power in wood sawing, J. Clean. Prod. 272 (2020), 122833, https://doi.org/10.1016/j.jclepro.2020.122833.
[31] X. Zhang, Y. Gao, Z. Guo, W. Zhang, J. Yin, W. Zhao, Physical model-based tool wear and break age monitoring in milling process, Mech. Syst. Signal Process. 184 (2023), 109641, https://doi.org/10.1016/j.ymssp.2022.109641.
[32] M. Nouri, B.K. Fussell, B.L. Ziniti, E. Linder, Real-time tool wear monitoring in milling using a cutting condition independent method, Int. J. Mach. Tools Manuf. 89 (2015) 1–13, https://doi.org/10.1016/j.ijmachtools.2014.10.011.
[33] O. Hatt, P. Crawforth, M. Jackson, On the mechanism of tool crater wear during titanium alloy machining, Wear 374 (2017) 15–20, https://doi.org/10.1016/j.wear.2016.12.036.
[34] B. Wu, M. Li, D. Ma, The flow behavior and constitutive equations in isothermal com pression of 7050 aluminum alloy, Mater. Sci. Eng. A 542 (2012) 79–87, https://doi.org/10.1016/j.msea.2012.02.035.
[35] M. Pohl, M. Rose, Piezoelectric shunt damping of a circular saw blade with autonomous power supply for noise and vibration reduction, J. Sound Vib. 361 (2016) 20–31, https://doi.org/10.1016/j.jsv.2015.09.021.
[36] E. Kannatey-Asibu Jr., A transport-diffusion equation in metal cutting and its application to analysis of the rate of flank wear, J. Eng. Industry 107 (1985) 81–89, https://doi.org/10.1115/1.3185971.
[37] M. Ekevad, L. Cristovao, B. Marklund, Wear of teeth of circular saw blades, Wood Mater. Sci. Eng. 7 (3) (2012) 150–153, https://doi.org/10.1080/17480272.2012.669405.
[38] H. Sasahara, Y. Sukegawa, Y. Yamada, Cfrp machining capability by a circular saw, Precis. Eng. 52 (2018) 291–299, https://doi.org/10.1016/j.precisioneng.2018.01.005.
[39] B. Wang, Z. Liu, Investigations on deformation and fracture behavior of workpiece material during high speed machining of 7050-t7451 aluminum alloy, CIRP J. Manuf. Sci. Technol. 14 (2016) 43–54, https://doi.org/10.1016/j.cirpj.2016.05.007.
[40] B. Wang, Z. Liu, Acoustic emission signal analysis during chip formation process in high speed machining of 7050-t7451 aluminum alloy and inconel 718 superalloy, J. Manuf. Process. 27 (2017) 114–125, https://doi.org/10.1016/j.jmapro.2017.04.003.